

1
2
3
4
5
6
7
8
9
10
11
12
13
14
15
16
17
18
19
20
21
22
23
24
25

**COMPARISON OF TWO MATHEMATICAL MODELS FOR CORRELATING
THE ORGANIC MATTER REMOVAL EFFICIENCY WITH HYDRAULIC
RETENTION TIME IN A HYBRID ANAEROBIC BAFFLED REACTOR
TREATING MOLASSES**

S. Ghaniyari-Benis^a, A. Martín^b, R. Borja^c *, M.A. Martín^b & N. Hedayat^d

^a Department of Chemical and Petroleum Engineering, Sharif University of Technology (SUT), P.O. Box 11365-8639, Tehran, Iran.

^b Departamento de Química Inorgánica e Ingeniería Química, Facultad de Ciencias, Campus Universitario de Rabanales, Edificio C-3, Ctra. Madrid-Cádiz, Km 396, 14071-Córdoba, Spain.

^c Instituto de la Grasa (C.S.I.C.), Avda. Padre García Tejero, 4, 41012-Sevilla, Spain.

^d School of Chemical Engineering, University of Tehran, P.O. Box 11155-4563, Tehran, Iran.

* Corresponding author: R. Borja (Tel.: +34 95 4689654; fax: +34 95 4691262; E-mail address: rborja@cica.es (R. Borja).

26

27

28

ABSTRACT

29

30 A modelling of the anaerobic digestion process of molasses was conducted in a 70-
31 litre multistage anaerobic biofilm reactor or hybrid anaerobic baffled reactor with six
32 compartments at an operating temperature of 26 °C. Five hydraulic retention times (6,
33 16, 24, 72 and 120 h) were studied at a constant influent COD concentration of 10000
34 mg/L. Two different kinetic models (one was based on a dispersion model with first-
35 order kinetics for substrate consumption and the other based on a modification of the
36 Young equation) were evaluated and compared to predict the organic matter removal
37 efficiency or fractional conversion. The first-order kinetic constant obtained with the
38 dispersion model was 0.28 h^{-1} , the Peclet dispersion number being 45, with a mean
39 relative error of 2%. The model based on the Young equation predicted the behaviour of
40 the reactor more accurately showing deviations lower than 10% between the theoretical
41 and experimental values of the fractional conversion, the mean relative error being 0.9%
42 in this case.

43

44 **Keywords:** Anaerobic digestion - Modelling - Hydraulic retention time - Organic
45 matter removal efficiency - Hybrid anaerobic baffled reactor.

46

47

48

49

50

51

52 INTRODUCTION

53

54 Anaerobic digestion of wastewaters has been considered to have a number of
55 advantages over the conventional aerobic process. It saves the energy needed for
56 aeration, converts organic matter into methane gas, a readily useable fuel, needs low
57 nutrient requirement and produces low biomass. Anaerobic processes have gained
58 popularity over the past decade, and have already been applied successfully for the
59 treatment of many high and medium strength industrial wastewaters [1-7].

60 Taking into consideration the slow growth rate of many anaerobic microorganisms,
61 particularly methanogenics, the main objectives of the efficient reactor design must be
62 high retention time of cells with very little loss of microorganisms from the bioreactor.
63 The technological challenge to improve the anaerobic digestion lies in enhancing the
64 bacterial activity together with good mixing to ensure a high rate of contact between the
65 cells and their substrate [1, 3, 7].

66 The anaerobic baffled reactor (ABR) consists of a cascade of baffled
67 compartments where the wastewater flows upward through a bed of anaerobic sludge
68 after being transported to the bottom of the compartment. The ABR does not require the
69 sludge to granulate in order to perform effectively, although granulation can occur over
70 time [8, 9]. Experiments with lab-scale reactors have shown that the ABR is very stable
71 under shock loads due to its compartmentalised structure [9-11]. In addition, the ABR
72 has many potential advantages, i.e. no requirement of biomass with unusual settling
73 properties and low capital and operating costs coupled with mechanical simplicity [9].

74 In the present study, a hybrid anaerobic baffled (HABR) reactor or multistage
75 biofilm reactor with six compartments was used. This reactor configuration can be

76 considered as a combination of the anaerobic baffled reactor (ABR) and upflow
77 anaerobic fixed bed (UAFB) system. The upflow anaerobic filter basically is a contact
78 process in which wastes pass over or through a mass of biological solids contained
79 within the reactor by a fixed media [12]. The biomass in the reactor is attached to the
80 media surfaces as a thin biofilm, is entrapped within the media matrix, or is held as a
81 granulated or flocculated sludge mass beneath the media. Soluble organic compounds
82 in the influent wastewater pass in close proximity to this biomass and diffuse into the
83 surfaces of the attached or granulated solids where they are converted to intermediates
84 and end products, specifically, methane and carbon dioxide [12].

85 Therefore, the main properties of the HABR are: lower sludge yields, and the
86 ability to partially separate between the various phases of anaerobic catabolism [9-
87 11,13]. The latter causes a shift in bacterial population allowing increased protection
88 against toxic materials and higher resistance to changes in environmental parameters
89 such as pH and temperature. The greatest advantage of this reactor configuration is
90 probably its ability to separate acidogenesis and methanogenesis longitudinally down
91 the reactor, allowing the reactor to behave as a two-phase system without the associated
92 control problems and high costs.

93 Kinetic studies are very helpful for reproducing the operational behaviour of the
94 anaerobic process and understanding the metabolic routes of biodegradation, while
95 simultaneously saving time and money [14]. However, the development of an up-to-
96 date model of organic matter anaerobic degradation is complex with considerable
97 difficulties due to the high number of variables affecting the anaerobic system [15, 16].
98 For instance, it is difficult to describe the whole anaerobic process by reliable kinetics
99 since hydrolysis of complex insoluble substrate depends on many different parameters
100 such as particle size, production of enzymes, pH and temperature [17].

101 A model was developed for the anaerobic digestion of a glucose-based medium in
102 an innovative high-rate reactor known as the periodic anaerobic baffled reactor (PABR).
103 In this model, each compartment is considered as two variable volume interacting
104 sections, with constant total volume, one compartment with high solids and the other
105 one with low solid concentrations, with the gas and liquid flows influencing the material
106 flows between the two sections. For the simulation of glucose degradation, the biomass
107 was divided into acidogenic, acetogenic and methanogenic groups of microorganisms.
108 The model succeeded in predicting the reactor performance as the organic loading rate
109 was gradually increased [18]. Another kinetic model for predicting the behaviour of the
110 PABR was developed based on batch experiments using glucose as substrate [8]. The
111 PABR may be operated as an upflow anaerobic sludge blanket (UASB) reactor, an ABR
112 or at an intermediate mode. The key assumption of this model was that the hydraulic
113 behaviour of a PABR was equivalent to the behaviour of CSTRs in series as regards the
114 dissolved matter. The model adequately predicted the experimental behaviour of this
115 glucose-fed PABR and was also used to examine the performance of this reactor as a
116 function of the operating conditions, both for constant and varying loading rates. It was
117 shown that the reactor would best be operated as a UASB or an ABR [8].

118 Another kinetic model was recently developed for explaining the performance of a
119 four-compartment ABR, incorporating granular sludge biomass and operating at
120 different hydraulic retention times (HRT) in the range of 3 to 24 hours using dilute
121 aircraft de-icing fluid with total chemical oxygen demand (COD) concentrations in the
122 range of 300-750 mg/L. However, the first-order empirical model initially developed for
123 describing the reactor performance did not adequately predict the total COD removal
124 efficiency in the reactor providing inconsistent results for the kinetic coefficient values

125 and no predictive correlation of these coefficients with substrate concentration,
126 hydraulic retention time and organic loading rate could be achieved [19, 20].

127 A mathematical model of the baffled reactor performance was developed and
128 applied using a concept of completely mixed reactors operating in series to describe the
129 performance of a modified laboratory-scale (150 L) ABR using molasses wastewater as
130 substrate [21]. This reactor had three chambers and a final settler. The first two
131 compartments each had a 10 cm layer of plastic media (Pall rings with a specific surface
132 area of $142 \text{ m}^2/\text{m}^3$) near the liquid surface. The third chamber had the upper half filled
133 with a modular corrugated block. This kinetic analysis focussed on the granular sludge
134 bed, with total mass of granular sludge as the main parameter. The model results were
135 in good agreement with the experimental data [21].

136 The Young model has been recently used to obtain the kinetic parameters of the
137 anaerobic digestion of synthetic domestic sewage in an upflow filter with corrugated
138 plastic rings as packing media at psychrophilic temperature (15-17 °C). The flow pattern
139 observed in this reactor was intermediate between plug-flow and CSTR system,
140 although the plug-flow was predominant in this case [7].

141 However, despite the advantages offered by the hybrid anaerobic baffled reactors,
142 few mathematical analyses have been reported to date for modelling the kinetic
143 behaviour of these reactors and none of them for simulating the variation of the total
144 COD removal efficiency under several HRTs. Therefore, the main objective of this
145 work was to compare two different kinetic models in the anaerobic treatment of
146 molasses as a source of carbon: a model based on the concept of an axial diffusion or
147 dispersion model with first-order kinetics for substrate consumption and a model based
148 on a modification of the Young equation. These mathematical models have not to date
149 been reported in the literature as describing the kinetic performance of this specific type

150 of hybrid reactor operating under varying HRTs. The anaerobic hybrid reactor used for
151 this purpose was composed of six sequential compartments, where each one formed a
152 packed bed using Raschig rings as a medium for supporting the biofilm formation.

153

154

155 **MATERIALS AND METHODS**

156 *Laboratory-scale experimental set-up*

157 The hybrid anaerobic baffled reactor was composed of six discrete compartments with a
158 total working volume of 70 L. The six compartments were made from “Plexiglas” with
159 identical geometric characteristics, a total volume of 12 L and a gas accumulation space
160 of 0.75 L for each one. The baffles inside the reactor were used to direct the flow of
161 wastewater in an upflow mode through a series of compartments where each one
162 formed a packed bed using Raschig Rings as a media to support the biofilm formation.
163 The main characteristics of this Raschig Ring packing were: material, metal; nominal
164 size, 13 mm; height, 25 mm; wall thickness, 0.8 mm; surface area, 420 m²/m³; and 85%
165 porosity. The porosity of the beds was 81% and the fixed beds were placed up to a
166 height of 40 cm from the bottom of the reactor. The beds maintained 73% porosity after
167 cell immobilization. A schematic diagram of the experimental set-up used, including
168 some reactor details, are shown in Figure 1.

169 The reactor was thermostated with a water jacket which kept the operational
170 temperature at 26 ± 0.5°C, and effluent wastewater from the sixth compartment was
171 discharged. The six compartments operated only in an anaerobic regime. Sampling taps
172 provided on the wall of each compartment allowed extraction of samples for analysis in
173 various chambers of the biofilm reactor.

174

175 *Molasses used*

176 The reactor was fed with molasses as a carbon source. The characteristics of the
177 molasses used are summarized in Table 1. During the start-up period, ammonium
178 phosphate and urea were used as sources of phosphorus and nitrogen, respectively.
179 Micronutrients and trace metals, with the characteristics and composition shown in
180 Table 2, were also added during the start-up period. During the start-up period, the
181 COD:N:P ratio was 100:5:1. When a steady-state condition was achieved, the COD:N:P
182 ratio was changed to 350:5:1. In order to neutralize any volatile fatty acids (VFA)
183 accumulation and prevent acid zone forming in the reactor, sodium bicarbonate was
184 used as an alkalinity supplement. Given the appropriate pH of the influent used as feed
185 (7.4) the volume of the sodium bicarbonate solution added was very small in all cases.
186 This solution was only added during the start-up period.

187

188 *Inoculum and experimental procedure*

189

190 The microorganisms used as inoculum in the reactor came from the sludge of a lab-scale
191 ANAMMOX (Anaerobic Ammonium Oxidation)-AFBR (Anaerobic Fluidized Bed
192 Reactor) system. The reactor was initially seeded with 27 L of anaerobic sludge. The
193 basic characteristics of the inoculum used were: 1857 mg/L of total nitrogen, 967 mg/L
194 of ammonia nitrogen, a total acidity of 367 mg acetic acid/L; 96 g/L of total solid
195 content, 40 g/L of volatile solid content, 1.898 g CaCO₃/L of bicarbonate alkalinity and
196 a pH of 6.8.

197 At the beginning of the experiments, for effective biofilm formation on the support
198 media, the reactor was initially started by increasing the organic loading rate from 0.5 to
199 2.5 g COD/L per day in a fed-batch mode. Molasses were used as substrate during this
200 step. After a batch feeding period of two months, this same influent was used as a

201 second feeding step in continuous mode at a constant organic loading rate of 4 g
202 COD/L·d for another period of two months.

203 The reactor was operated until a steady-state performance was reached. The
204 bioreactor was subjected to increasing HRTs and the performance of the system was
205 evaluated. Five HRTs (0.25, 0.67, 1, 3 and 5 days, equivalent to 6, 16, 24, 72 and 120
206 hours, respectively) were studied at a constant influent COD concentration of 10000
207 mg/L.

208

209 *Analytical Methods*

210 The COD concentration was measured by using a semi-micro method [22]. This method
211 was very effective for COD determinations in samples with high salinity, organic matter
212 content and nitrogenous compounds. Total VFA (TVFA) concentrations in the samples
213 were analyzed using a titrimetric method [23]. Ammonia-nitrogen was detected by the
214 4500-NH₃D method, with a NH500/2 WTW ion selective electrode and WTW pH
215 320m. Electrodes were calibrated according to the manufacturer's procedures. BOD was
216 measured according to standard methods [23]. Daily liquid samples were withdrawn
217 and centrifuged at 13000 rpm for 8 min until a clear supernatant was obtained.

218 The steady-state values of operational parameters were taken as the average of seven
219 successive measurements for those parameters when the deviations between the values
220 were less than 3% in all cases.

221

222 *Software used*

223 SigmaPlot software (version 11.0) was used to elaborate all the graphs and Figures of
224 this study and to perform the statistical analyses. Mathcad software (version 14) was
225 used to solve the mathematical equations corresponding to the two models assessed.

226

227

228 **RESULTS AND DISCUSSION**

229 *Operational Performance of the HABR*

230 Figure 2 shows the variation of the pH within the different compartments of the reactor
231 for all the HRTs studied. As can be seen, in all cases the process takes place within the
232 most appropriate pH values for an adequate and stable anaerobic digestion [24]. An
233 increase in pH values was observed from the first to the sixth compartments for all
234 HRTs assessed. In addition, for a same step or compartment, the pH increased at higher
235 HRTs. In compartments 1 and 2, and mainly at HRTs of 6 h and 16 h, acidogenesis
236 prevailed over methanogenesis. The same behaviour was observed in compartment 3 at
237 an HRT of 6 h. At HRTs of 72 h and 120 h and after compartment 3, pH values were
238 always higher than 7.2.

239 In relation to the variations profile of TVFA concentration (Figure 3), it was
240 observed that for all HRTs studied, the TVFA values dropped from the first to the sixth
241 compartments. At an early stage in the process where the growth rate of acetogens is
242 higher and the methanogens have not yet grown enough, the TVFA values are high.
243 However, with the passing of time (once steady-state conditions were achieved) and an
244 increase in the growth of methanogens, the TVFA values dropped with increasing HRT,
245 and the TVFA values decreased in all chambers. At HRTs of 24 h, 72 h and 120 h and
246 after compartment 4, the TVFA concentrations were very low, which demonstrated the
247 almost total transformation of the organic matter into methane. At HRTs of 6 h and 16 h
248 and for the two first compartments, the TVFA concentration was higher than 2000
249 mg/L, which coincides with the lower pH values observed in these two first steps
250 (Figure 2). This shows that by reducing the contact time between the molasses and the

251 biomass, there was not enough time to transform the TVFAs to end products and the
252 outflow COD was basically constituted by volatile fatty acids.

253 TVFA concentrations in effluents of a multistage anaerobic migrating blanket
254 reactor (AMBR) increased from 25 to 182 mg/L as the HRT decreased from 10.3 days
255 to 1 day when treating synthetic wastewater containing glucose as a carbon source [25].
256 This AMBR reactor consisted of a rectangular tank with an active volume of 13.5 L,
257 which was divided into three compartments, which were mixed equally every 15
258 minutes at 60 rpm to ensure gentle mixing. Comparing these data with those obtained in
259 the present work, it can be seen that similar TVFA values (210 mg/L) were obtained in
260 the effluents of the HABR reactor at an HRT of 24 h.

261

262 *Mathematical modelling*

263 The fractional conversion or organic matter removal efficiency (per one) can be defined
264 as the ratio between the amount of COD eliminated and the COD fed [26]. Figure 4
265 shows the evolution of the fractional conversion (X) with the HRT (h). Because the
266 reactor has 6 compartments (equivalent to 6 stages), each stage involves a partial HRT
267 and, thus, a partial conversion. Therefore, the total number of experimental points
268 (partial HRTs) plotted in Figure 4 is equal to 30 (6 stages x 5 partial HRTs/stage). As
269 can be seen, for HRTs in the interval of 0 h-20 h the conversion increased drastically
270 with increasing HRTs. For HRTs higher than 20 h the increase in the conversion with
271 HRT is slower with a tendency towards an asymptotic value, without reaching total
272 conversion at a HRT as high as 120 h. This fact demonstrated the occurrence of a small
273 fraction of the substrate that is non-biodegradable anaerobically.

274 In order to predict the fractional conversion or organic matter removal efficiency
275 (per one) for HABR, two different models were evaluated and compared: an axial

276 diffusion or dispersion model and an empirical model based on a modification of the
277 Young model [12].

278

279 *Axial diffusion or dispersion model with first-order kinetics for substrate consumption*

280 The formulation of a mathematical model for a complex system such as that used in the
281 present work, in which both the overall kinetics and the flow pattern influence the
282 process, makes necessary to assume certain significant hypotheses that allow to
283 harmonize the model precision with its possible usefulness.

284 To study the kinetics of the biological reactions, a Michaelis-Menten type model has
285 been widely proposed [27]:

$$286 \quad (-r_S) = k \cdot S / (K_S + S) \quad (1)$$

287 where: r_S is the substrate consumption rate, S is the substrate concentration, k is the
288 kinetic constant and K_S is the saturation constant.

289 For low substrate concentrations, $K_S \gg S$, and equation (1) is reduced to a first
290 order equation: $(-r_S) = k_I \cdot S$, where k_I is a first-order kinetic constant.

291 Equation (1) has been previously proposed for anaerobic digestion of complex
292 substrates or wastewaters with high suspended solid content, which require a hydrolysis
293 step previous to its acidification [27-30].

294 In order to describe the biological reaction within each compartment of the reactor it
295 is necessary to know the kinetic equation as well as the flow pattern. As a first
296 approximation and given that mixing is not deliberately promoted in each step, it could
297 be considered that the flow could behave as an ideal a “piston flow” or plug-flow.
298 However, it should be taken into consideration that biogas generation causes an airlift
299 effect within each compartment resulting in a certain mixing. As a consequence it is

300 reasonable to assume that the real flow must behave as an intermediate between
301 completely stirred and plug-flow.

302 This physical situation can approximately be described by an axial or dispersion
303 model [26, 31]. Assuming first-order kinetics for substrate consumption, the following
304 equation was proposed for the calculation of the fractional conversion [26, 32]:

$$305 \quad X = 1 - [4 \cdot a \cdot \exp(u \cdot L / (2 \cdot D)) / [(1 + a)^2 \cdot \exp(a \cdot u \cdot L / (2 \cdot D)) - (1 - a)^2 \cdot \exp(-a \cdot u \cdot L / (2 \cdot D))]] \quad (2)$$

306 where:

$$307 \quad a = [1 + 4 \cdot k_l \cdot HRT \cdot (D / (u \cdot L))]^{0.5} \quad (3)$$

308 and X is the fractional conversion, u is the linear velocity, L is the bioreactor length, D
309 is the diffusion constant, HRT is the hydraulic retention time, and k_l is the first-order
310 reaction rate constant. The term $(D / (u \cdot L))$ is the dimensionless dispersion number and its
311 value is a function of the mix level in the reactor and its geometry. The inverse of the
312 dimensionless dispersion number $((u \cdot L) / D)$ is known as the Peclet group or Peclet
313 number [32].

314 A detailed scheme of the different steps made for the calculation of the first-order
315 kinetic constant (k_l) and dispersion number $(D / (u \cdot L))$ is shown in the flow diagram
316 included in Figure 5. Following this diagram for the calculation, the values obtained for
317 k_l and $(D / (u \cdot L))$ were 0.28 h^{-1} and 45, respectively.

318 The following equation was used as the analytical criterion for determining the
319 ending of the calculation and consequently to determine the optimum values of the
320 kinetic constant and dispersion number of the process:

$$321 \quad \epsilon = [(\Sigma(X_{exp} - X_{model}) / X_{exp})^2]^{1/2} / N \quad (4)$$

322 where X_{exp} and X_{model} are the experimental and theoretical conversion values
323 respectively, the latter being calculated by using equations (2) and (3) using the

324 Mathcad software (version 14), C is the mean relative error of the fractional conversion,
325 its value being 0.02, and N is the number of experimental points ($N=30$).

326 As can be seen in Figure 4, only for fractional conversions higher than 0.8, slight
327 deviations between the experimental and theoretical conversion values were observed.
328 These deviations could be due to the increase in the experimental effluent CODs caused
329 by the endogenous metabolism, which provokes a reduction of the experimental
330 conversion. The proposed dispersion model (with first-order kinetics) was validated by
331 comparing the experimental fractional conversion data with the theoretical values
332 obtained with this model for all HRTs studied. Figure 6 shows a comparison of the
333 experimental and simulated data obtained with this model for all experiments carried
334 out. As can be seen, deviations equal to or lower than 20% between the experimental
335 and theoretical fractional conversion values were obtained. This demonstrates the
336 suitability of the proposed model to represent the performance of the HABR and,
337 therefore, that the global or overall kinetic parameter obtained approximately represents
338 the activity of the different microorganism populations or microbial communities
339 involved in the anaerobic process.

340 On the other hand, the value of the kinetic constant, k_I , obtained with this model in
341 the present work (0.28 h^{-1}) is higher than the specific substrate utilization rate
342 coefficient obtained in an ABR with three chambers (0.012 h^{-1}) processing molasses
343 wastewater (9-38 g COD/L) at OLRs of between 5-25 kg COD/m³ d [21]. However, this
344 constant value is lower than the maximum specific rate of substrate consumption (0.70
345 h^{-1}) achieved in the methanogenesis from acetate using a periodic ABR under increasing
346 organic loading conditions (2700 to 10500 mg/L) [18].

347 In addition, a dispersion model was also found to be highly suitable for describing
348 the anaerobic digestion of municipal wastewater in a novel outside cycle reactor

349 developed based on the characteristics of an expanded granular sludge bed (EGSB)
350 reactor [26]. The standard deviation of the simulated data (concentration of the effluent
351 suspended solids) was less than 6% [33]. The flow pattern and behaviour of an
352 acidogenic UASB reactor was also successfully simulated with the dispersion model.
353 The axial dispersion number was identified as the most important factor in the
354 dispersion modelling of this reactor [34]. The axial dispersion model was also found to
355 be appropriate for studying the hydrodynamic pattern of a fluidised bed reactor [35] and
356 a rotating disc anaerobic reactor digesting acetic acid as substrate [36]. The feasibility of
357 the dispersion model simulating the process performance in anaerobic filters was also
358 reported in the literature [37].

359 According to Levenspiel [26] and taking into account the value of the dispersion
360 number obtained (45), the flow pattern in the present bioreactor is intermediate between
361 the plug-flow and completely stirred reactors, although it comes nearer to the
362 completely stirred model. Similar intermediate behaviour between plug-flow and ideally
363 mixed was also found in an ABR with eight compartments treating dilute wastewater
364 (500 mg COD/L) at HRTs in the range of 80-10 h [38].

365

366 *Empirical modified Young model*

367 Finally, the experimental results obtained (fractional conversion values, hydraulic
368 retention times) were fitted to the following empirical equation, which represents a
369 modification of the Young model [12]:

$$370 \quad X = a(1 - b/HRT^c) \quad (5)$$

371 where a , b and c are empirical constants derived from a non-linear adjustment of the
372 above-mentioned experimental value pairs (X_{exp} , HRT_{exp}) by using the least-squares
373 method.

374 By solving Equation (5) with the above mentioned Mathcad software, the following
375 values for these empirical constants were obtained: $a = 1.13$; $b = 0.73$ and $c = 0.29$.
376 Figure 7 shows a comparison of the experimental fractional conversion data with the
377 theoretical curve obtained using the modified Young model. Figure 8 shows a
378 comparison of the experimental fractional conversion values with the theoretical values
379 obtained with this proposed model represented by Equation (5). Because the mean
380 relative error was only 0.9%, a completely satisfactory fit was observed. This means
381 that the relative error was much lower than that obtained with the dispersion model
382 using first-order kinetics (2%). In addition, the Young model has three adjustment
383 mathematical parameters while the dispersion model has only one parameter, and the
384 higher the number of adjustment parameters, the better is the final adjustment.
385 Therefore, of the two models proposed, the modified Young model appears to match the
386 performance data more closely than the dispersion model hypothesis according to the
387 mean relative errors obtained in each adjustment. Accordingly the modified Young
388 model will be more suitable than the dispersion model to predict the behaviour of this
389 reactor under different operating conditions.

390

391

392 **CONCLUSIONS**

393

394 The operational behaviour of a hybrid anaerobic baffled reactor treating molasses was
395 assessed using two different kinetic models: a dispersion model with first-order kinetics
396 for substrate consumption and a modified Young model. These models were evaluated
397 and compared with the aim of simulating the organic matter removal or fractional
398 conversion under different HRTs.

399 The dispersion model reproduced the experimental results with a mean relative error
400 of 2%. The modified Young model allowed a better fit of the experimental results
401 showing a mean relative error of 0.9%.

402

403

404 **ACKNOWLEDGEMENTS**

405

406 The authors gratefully acknowledge the financial support of the Water Research Center
407 of Greentech (Co., Ltd.), Shiraz and the R&D Center of Anshan Corporation. The
408 authors also thank Dr. Daryoush Mehrparast and Dr. Anahita Parsnejad for their help.

409

410

411 **REFERENCES**

412

- 413 1. Mosquera-Corral A, Belmar A, Decap J, Sossa K, Urrutia H, Vidal G (2008)
414 Anaerobic treatment of low-strength synthetic TCF effluents and biomass adhesion
415 in fixed-bed systems. *Bioprocess Biosyst Eng* 31:535-540.
- 416 2. Song KG, Cho J, Ahn KH (2009) Effects of internal recycling time mode and
417 hydraulic retention time on biological nitrogen and phosphorus removal in a
418 sequencing anoxic/anaerobic membrane bioreactor process. *Bioprocess Biosyst Eng*
419 32:135-142.
- 420 3. Diamantis V, Aivasidis A (2010) Two-stage UASB design enables activated-sludge
421 free treatment of easily biodegradable wastewater. *Bioprocess Biosyst Eng* 33:287-
422 292.

- 423 4. Tawfik A, El-Gohary F, Temmink H (2010) Treatment of domestic wastewater in
424 an up-flow anaerobic sludge blanket reactor followed by moving bed biofilm
425 reactor. *Bioprocess Biosyst Eng* 33:267-276.
- 426 5. Gómez X, Cuetos MJ, Tartakovsky B, Martínez-Nuñez MF, Moran A (2010) A
427 comparison of analytical techniques for evaluating food waste degradation by
428 anaerobic digestion. *Bioprocess Biosyst Eng* 33: 427-438.
- 429 6. Ganesh R, Rajinikanth R, Thanikal JV, Ramanujam RA, Torrijos M (2010)
430 Anaerobic treatment of winery wastewater in fixed bed reactors. *Bioprocess Biosyst*
431 *Eng* 33:619-628.
- 432 7. Martin MA, De la Rubia MA, Martin A, Borja R, Montalvo S, Sánchez E (2010)
433 Kinetic evaluation of the psychrophilic anaerobic digestion of synthetic domestic
434 sewage using an upflow filter. *Bioresour Technol* 101:131-137.
- 435 8. Skiadas IV, Gavala HN, Lyberatos G (2000) Modelling of the periodic anaerobic
436 baffled reactor (PABR) based on the retaining factor concept. *Water Res* 34:3725-
437 3736.
- 438 9. Barber WP, Stuckey DC (1999) The use of the anaerobic baffled reactor (ABR)
439 for wastewater treatment: a review. *Water Res* 33:1559-1578.
- 440 10. Kuscu OS, Sponza DT (2006) Treatment efficiencies of a sequential anaerobic
441 baffled reactor (ABR)/completely stirred tank reactor (CSTR) system at increasing
442 p-nitrophenol and COD loading rates. *Process Biochem* 41:1484-1492.
- 443 11. Grover R, Marwaha SS, Kennedy JF (1999) Studies on the use of an anaerobic
444 baffled reactor for the continuous anaerobic digestion of pulp and paper mill black
445 liquors. *Process Biochem* 34:653-657.
- 446 12. Young JC (1991) Factors affecting the design and performance of upflow
447 anaerobic filters. *Water Sci Technol* 24:133-155.

- 448 13. Ghaniyari-Benis S, Borja R, Ali Monemian S, Goodarzi V (2009) Anaerobic
449 treatment of synthetic medium-strength wastewater using a multistage biofilm
450 reactor. *Bioresour Technol* 100:1740-1745.
- 451 14. Galí A, Benabdallah T, Astals S, Mata-Alvarez J (2009) Modified version of
452 ADM1 model for agro-waste application. *Bioresour Technol* 100:2783-2790.
- 453 15. Martín-Santos MA, Siles J, Chica AF, Martín A (2010) Modelling the anaerobic
454 digestion of wastewater derived from the pressing of orange peel produced in
455 orange juice manufacturing. *Bioresour Technol* 101:3909-3916.
- 456 16. Batstone DJ, Keller J, Newell RB, Newland M (2000) Modelling anaerobic
457 degradation of complex wastewater, I: model development. *Bioresour Technol*
458 75:67-74.
- 459 17. Weiland P (2010) Biogas production: current state and perspectives (mini-review).
460 *Appl Microbiol Biotechnol* 85:849-860.
- 461 18. Stamatelatou K, Lokshina L, Vavilin V, Lyberatos G (2003) Performance of a
462 glucose fed periodic anaerobic baffled reactor under increasing organic loading
463 conditions: 2. Model prediction. *Bioresour Technol* 88:137-142.
- 464 19. Marin J, Kennedy KF, Eskicioglu C, Hamoda MF (2007) Compartmental
465 anaerobic baffled reactor kinetic model for treatment of dilute aircraft de-icing
466 fluid. *Proceedings of the Third IASTED International Conference on*
467 *Environmental Modelling and Simulation*, EMS, Honolulu, Hawaii (USA), Ed. J
468 Wilson, Acta Press, August 20-22, pp. 58-63.
- 469 20. Kennedy K, Barriault M (2007) Treatment kinetics of aircraft deicing fluid in an
470 anaerobic baffled reactor. *J Environ Eng Sci* 6:11-17.
- 471 21. Xing J, Boopathy R, Tilche A (1991) Model evaluation of hybrid anaerobic
472 baffled reactor treating molasses wastewater. *Biomass Bioenergy* 5:267-274.

- 473 22. Soto M, Veiga MC, Mendez R, Lema JM (1989) Semi-micro COD determination
474 method for high salinity wastewater. *Environ Technol Lett* 10:541-548.
- 475 23. *Standard Methods for the Examination of Water and Wastewater* 20th ed (1998)
476 APHA, AWWA, WPCF, Washington, DC.
- 477 24. Fannin KF (1987) Start-up, operation, stability and control. In: DP Chynoweth, R
478 Isaacson, editors. *Anaerobic digestion of biomass*, London, UK: Elsevier, pp. 171-
479 196.
- 480 25. Kuscu OS, Sponza DT (2009) Kinetics of para-nitrophenol and chemical oxygen
481 demand removal from synthetic wastewater in an anaerobic migrating blanket
482 reactor. *J Hazard Mater* 161:787-799.
- 483 26. Levenspiel O (2002) Modelling in chemical engineering. *Chem Eng Sci* 57:4691-
484 4696.
- 485 27. Martín A, Borja R Banks CJ (1994) Kinetic model for substrate utilization and
486 methane production during the anaerobic digestion of olive mill wastewater and
487 condensation water waste. *J Chem Technol Biotechnol* 60:7-16.
- 488 28. Palmowski LM, Müller JA (2000) Influence of the size reduction of organic waste
489 on their anaerobic digestion. *Water Sci Technol* 41:155-162.
- 490 29. Borja R, Rincon B, Raposo F, Sanchez E, Martin A (2004) Assessment of kinetic
491 parameters for the mesophilic anaerobic biodegradation of two-phase olive
492 pomace. *Int Biodet Biodeg* 53:71-78.
- 493 30. Borja R, Martin A, Sanchez E, Rincon B, Raposo F (2005) Kinetic modelling of
494 the hydrolysis, acidogenic and methanogenic steps in the anaerobic digestion of
495 two-phase olive pomace (TPOP). *Process Biochem* 40:1841-1847.
- 496 31. Scott Fogler H (1999) *Elements of chemical reaction engineering*. Prentice Hall
497 Inc., Upper Saddle River, New Yersey, USA.

- 498 32. Wehner JF, Wilhelm RH (1956) Boundary conditions of flow reactor. Chem Eng
499 Sci 6:89-98.
- 500 33. Zhou X, Zhang Y, Zhang X, Jiang M (2009) Simulation of sludge settling
501 property in a novel outside cycle anaerobic reactor. Huagong Xuebao/CIESC
502 Journal 60:738-743.
- 503 34. Ren TT, Mu Y, Yu HQ, Harada H, Li YY (2008) Dispersion analysis of an
504 acidogenic UASB reactor. Chem Eng J 142:182-189.
- 505 35. Otton V, Hihn JY, Béteau JF, Delpéch F, Chérury A (2000) Axial dispersion of
506 liquid in fluidised bed with external recycling: two dynamic modelling approaches
507 with a view to control. Biochem Eng J 4:129-136.
- 508 36. Breithaupt T, Wiesmann U (1998) Concentration profiles in rotating disc reactors:
509 Their mathematical model for the anaerobic digestion of acetic acid including an
510 experimental verification. Acta Hydrochim Hydrobiol 16:288-295.
- 511 37. Tseng SK, Lin RT, Liao KL (1992) Verification of dispersion model on anaerobic
512 reaction simulation. Water Sci Technol 26:2377-2380.
- 513 38. Langenhoff AAM, Stuckey DC (2000) Treatment of dilute wastewater using an
514 anaerobic baffled reactor: Effect of low temperature. Water Res 15:3867-3875.
- 515
- 516
- 517
- 518
- 519
- 520
- 521
- 522

523
524
525
526
527
528
529
530
531
532
533
534
535
536
537
538
539
540
541
542
543
544
545
546
547

Table 1. Characteristics of the molasses used

pH	7.4
Chemical oxygen demand (COD)	10290 mg/L
Biochemical oxygen demand (BOD ₅)	3250 mg/L
Kjeldahl nitrogen	183 mg/L
Total phosphate	10 mg/L
Fe ²⁺	10 mg/L
Ca ²⁺	592 mg/L
K ⁺	32 mg/L
Alkalinity	2070 mg/L
Total solids (TS)/Volatile solids (VS) ratio	1.5

548

549 **Table 2.** Composition and characteristics of the micronutrients and trace elements

550 solution

551

552 $\text{CoCl}_2 \cdot 6\text{H}_2\text{O}$ 0.25 mg/L

553 H_3BO_3 0.05 mg/L

554 $\text{FeSO}_4 \cdot 7\text{H}_2\text{O}$ 0.5 mg/L

555 $\text{MnCl}_2 \cdot 4\text{H}_2\text{O}$ 0.5 mg/L

556 ZnCl_2 0.05 mg/L

557 CuCl_2 0.15 mg/L

558 $\text{Na}_2\text{MoO}_4 \cdot 2\text{H}_2\text{O}$ 0.01 mg/L

559 $\text{NiSO}_4 \cdot \text{H}_2\text{O}$ 0.02 mg/L

560 Na_2SeO_3 0.01 mg/L

561 $\text{AlCl}_3 \cdot 6\text{H}_2\text{O}$ 0.05 mg/L

562 $\text{MgSO}_4 \cdot 7\text{H}_2\text{O}$ 0.3 mg/L

563

564

565

566

567

568

569

570

571

572

573

574

FIGURE CAPTIONS

575

576 **Figure 1.** Schematic diagram of the experimental set-up used.

577 **Figure 2.** Profile of the pH variations for the different HRTs studied.

578 **Figure 3.** Profile of the TVFA variations for the different HRTs studied.

579 **Figure 4.** Variation of the experimental and theoretical values of the fractional
580 conversion (obtained with the dispersion model using a first-order kinetics
581 for substrate consumption) with the hydraulic retention time.

582 **Figure 5.** Flow diagram or detailed scheme of the different steps made for the
583 calculation of the dispersion number and kinetic constant in the dispersion
584 model.

585 **Figure 6.** Comparison of the experimental and theoretical values of the fractional
586 conversion (obtained with the dispersion model using a first-order kinetics
587 for substrate consumption) for all the experiments carried out.

588 **Figure 7.** Variation of the experimental and theoretical values of the fractional
589 conversion (obtained with the empirical modified Young model) with the
590 hydraulic retention time.

591 **Figure 8.** Comparison of the experimental and theoretical values of the fractional
592 conversion (obtained with the empirical modified Young model) for all the
593 experiments carried out.

594

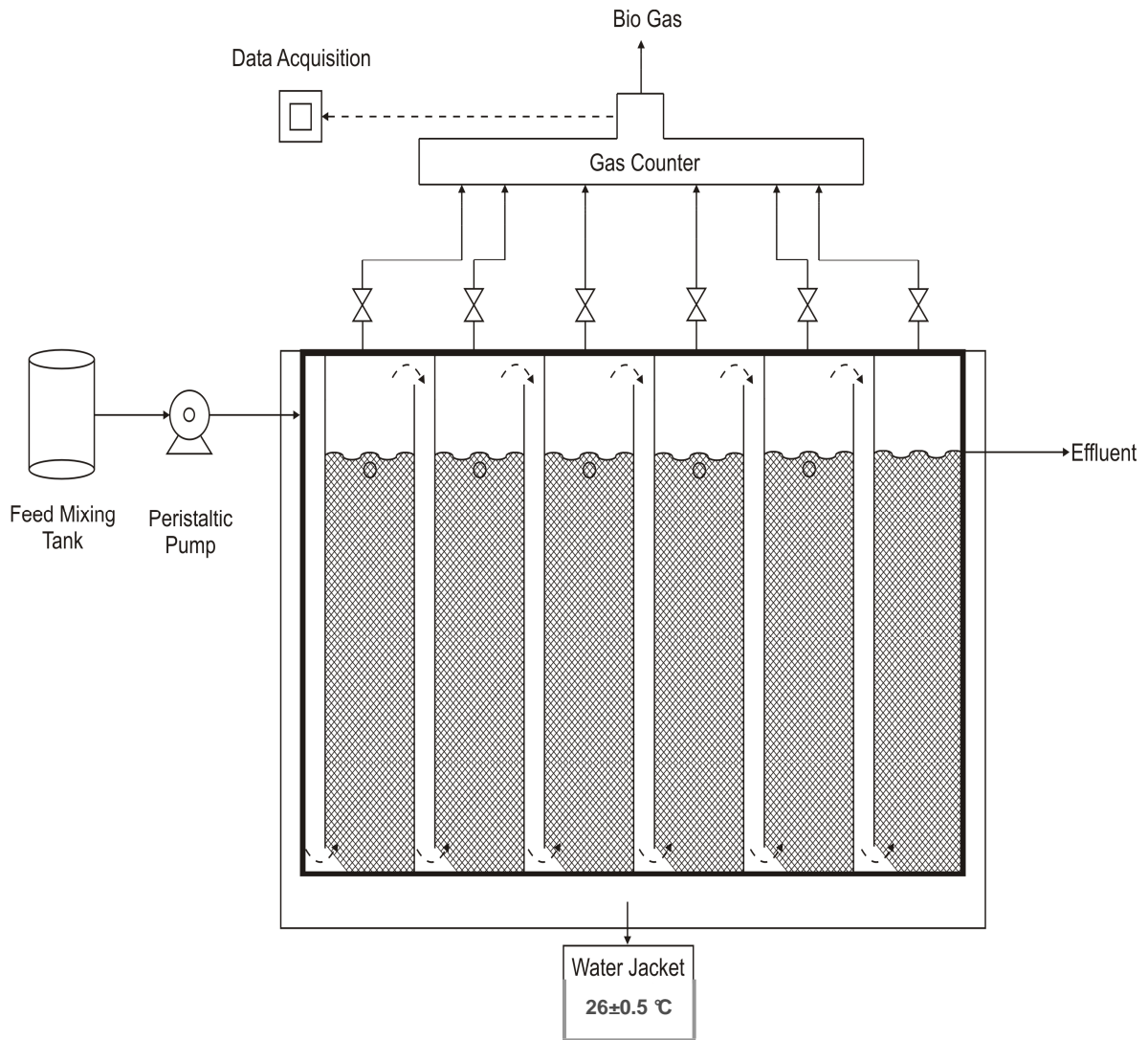
595

596

597

598 **Figure 1**

599
600
601
602
603
604
605
606
607
608
609
610
611
612
613
614
615
616
617
618
619
620
621
622
623



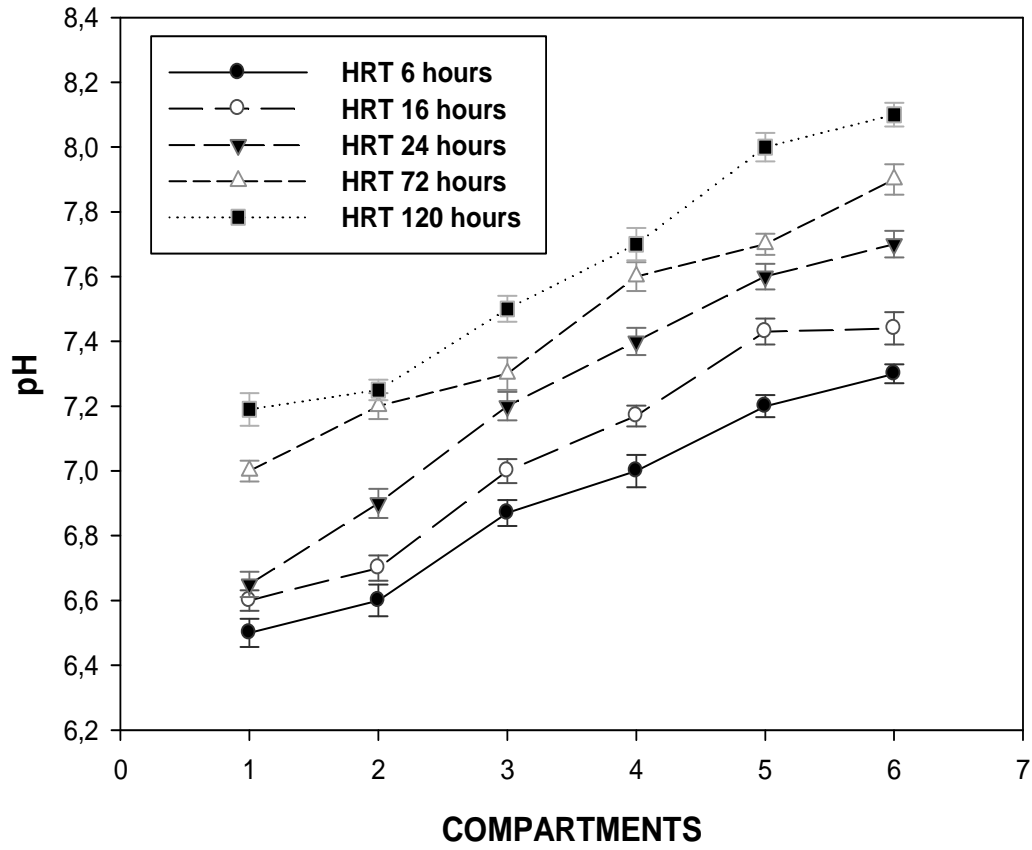


Figure 2

624
 625
 626
 627
 628
 629
 630
 631
 632
 633
 634
 635
 636
 637
 638
 639
 640
 641
 642
 643
 644
 645
 646
 647
 648
 649

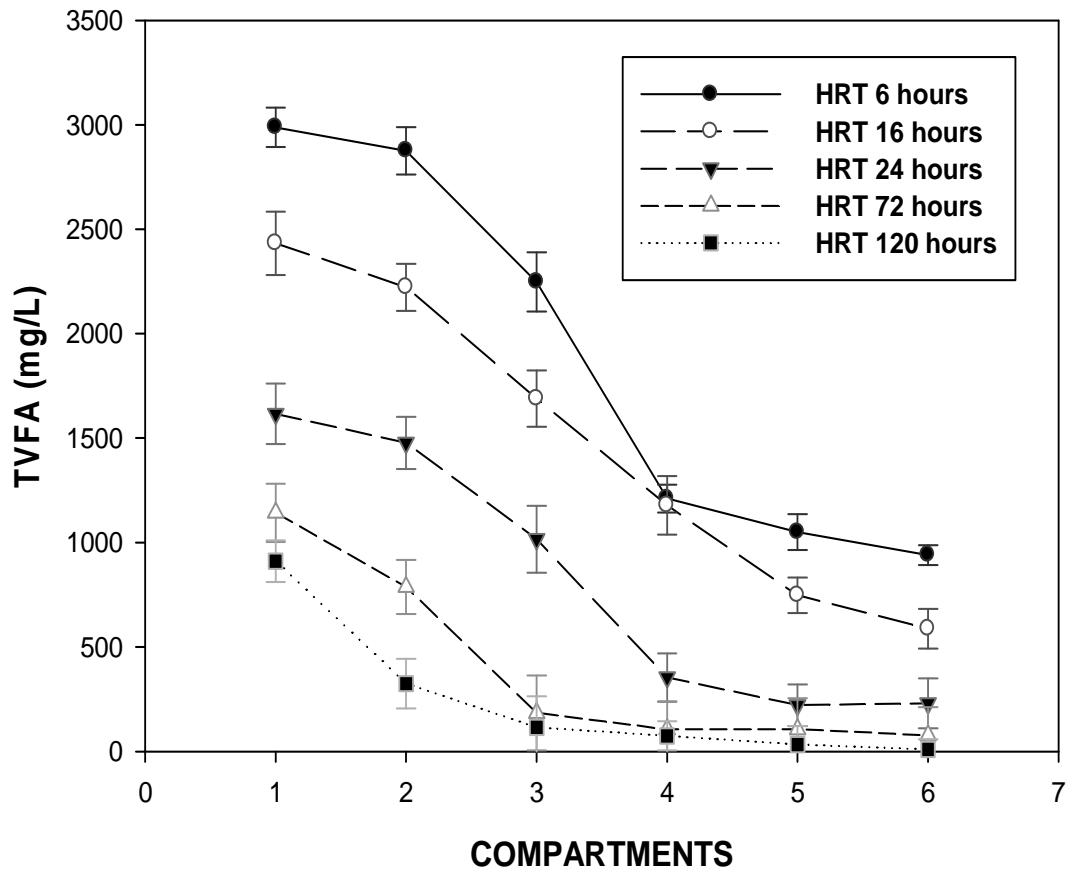


Figure 3

650
 651
 652
 653
 654
 655
 656
 657
 658
 659
 660
 661
 662
 663
 664
 665
 666
 667
 668
 669
 670
 671
 672
 673
 674

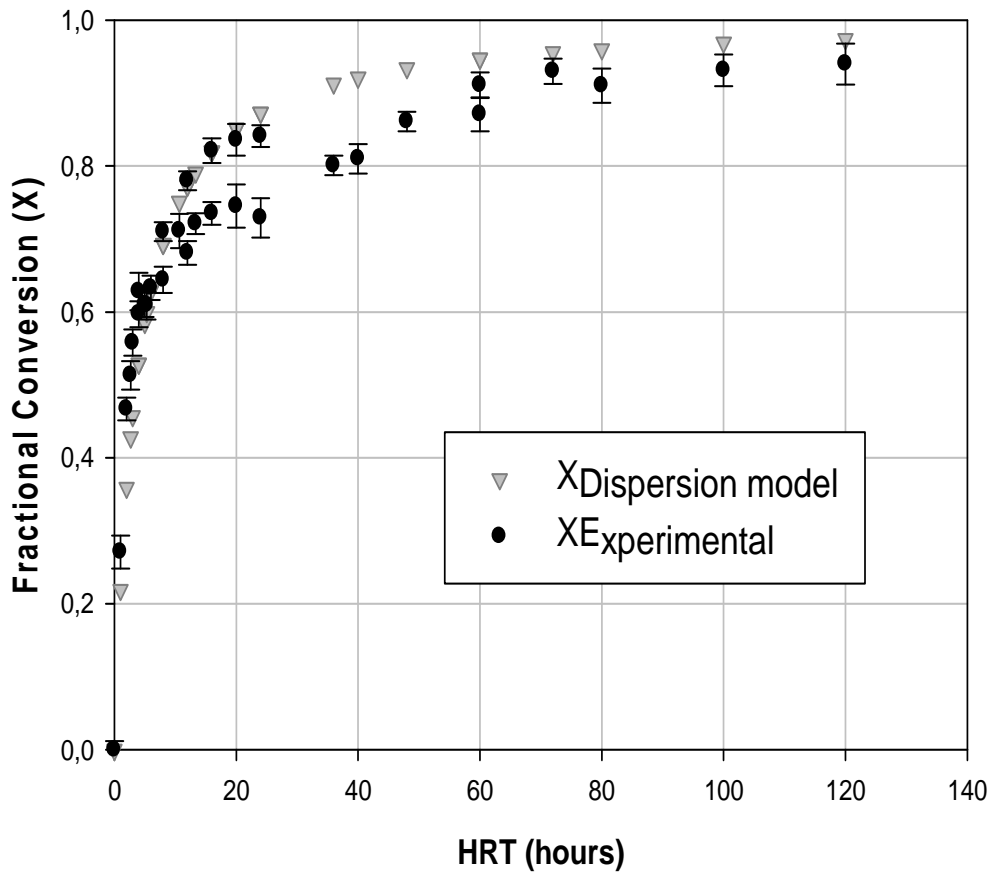
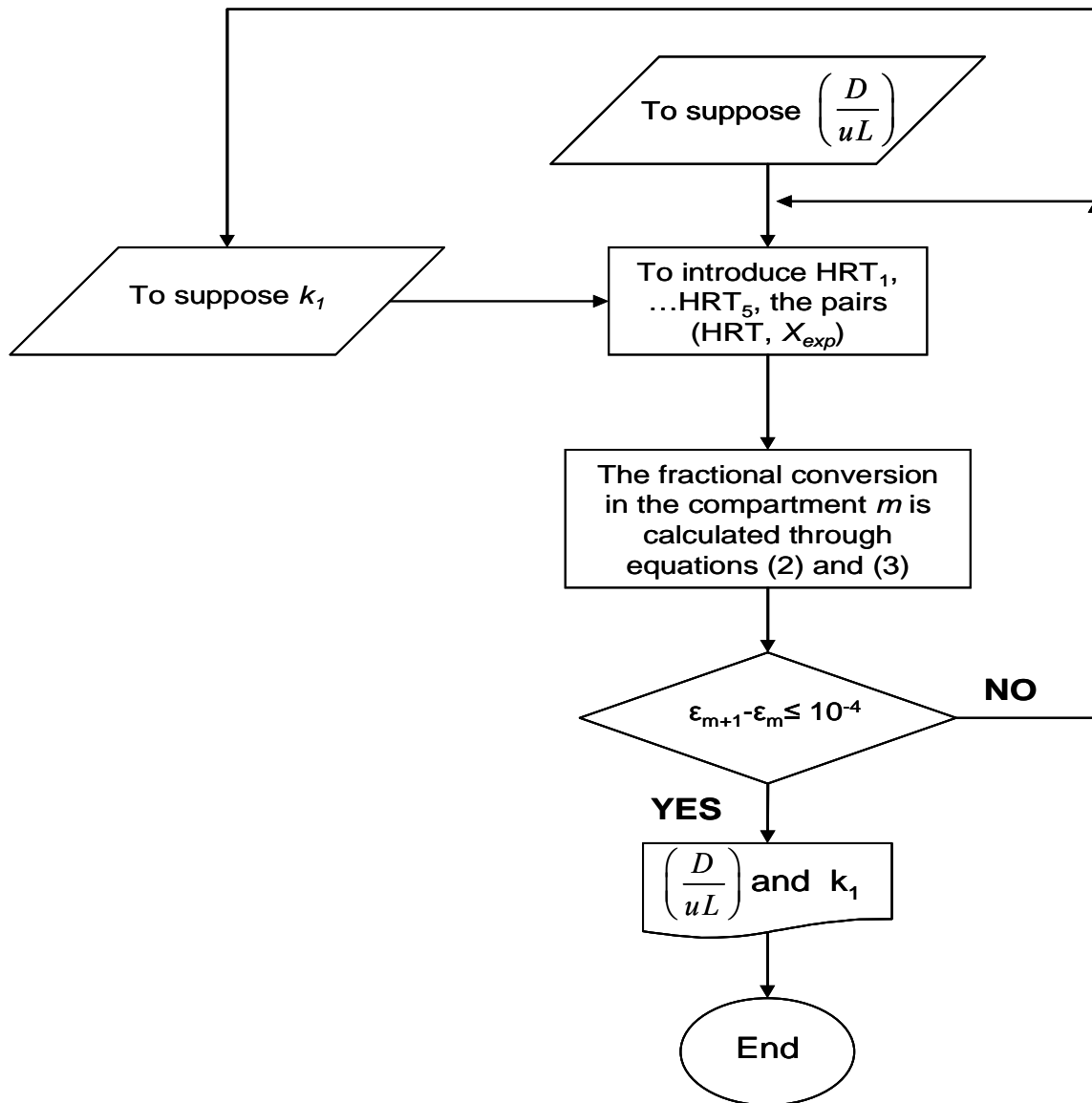


Figure 4

675
 676
 677
 678
 679
 680
 681
 682
 683
 684
 685
 686
 687
 688
 689
 690
 691
 692
 693
 694
 695
 696
 697
 698



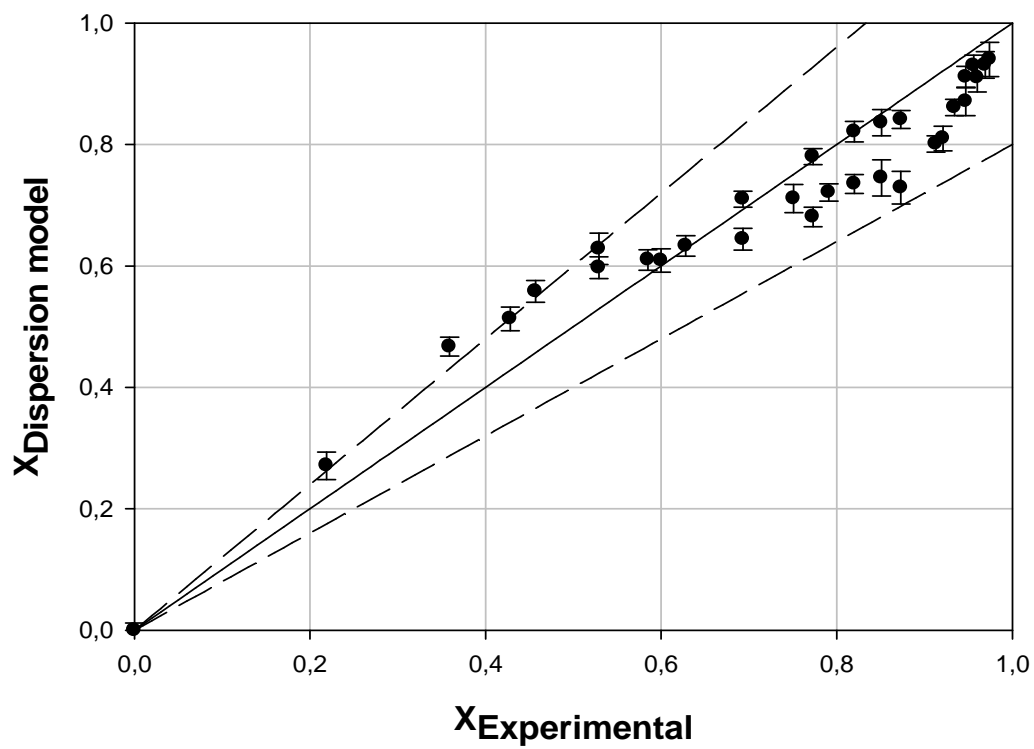


Figure 6

700
 701
 702
 703
 704
 705
 706
 707
 708
 709
 710
 711
 712
 713
 714
 715
 716
 717
 718
 719
 720
 721
 722

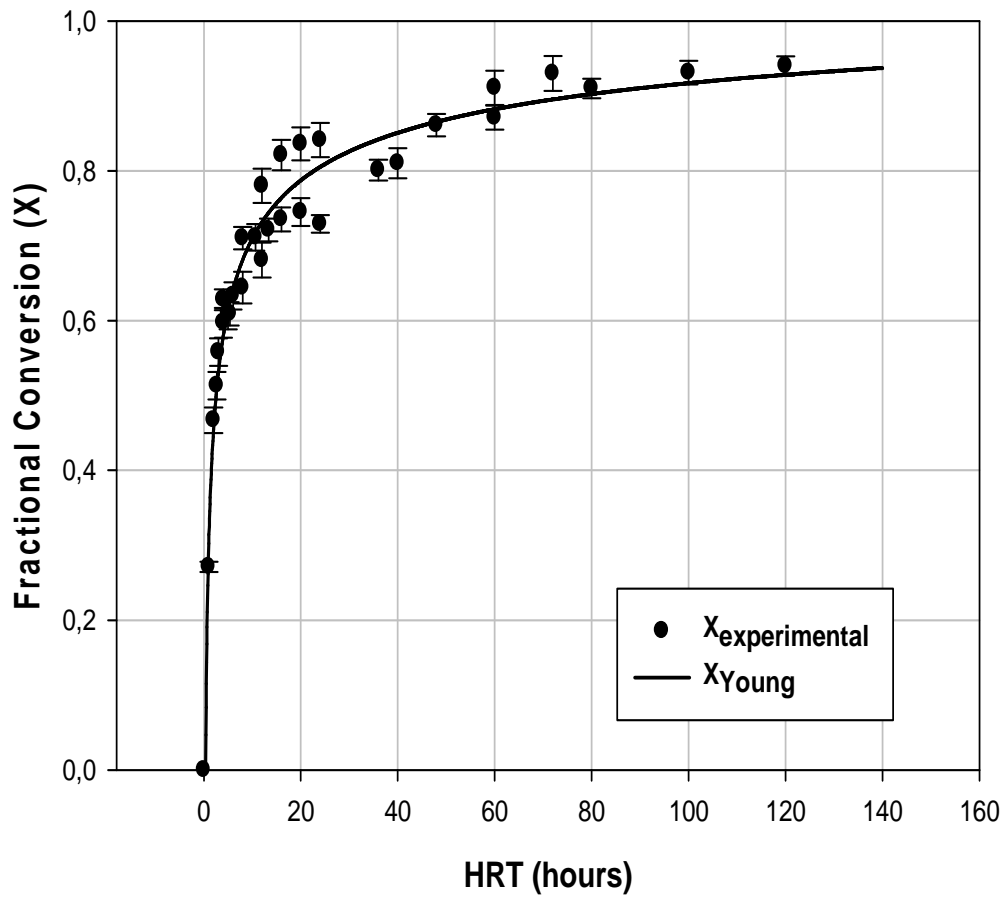


Figure 7

723
 724
 725
 726
 727
 728
 729
 730
 731
 732
 733
 734
 735
 736
 737
 738
 739
 740
 741
 742
 743
 744
 745
 746

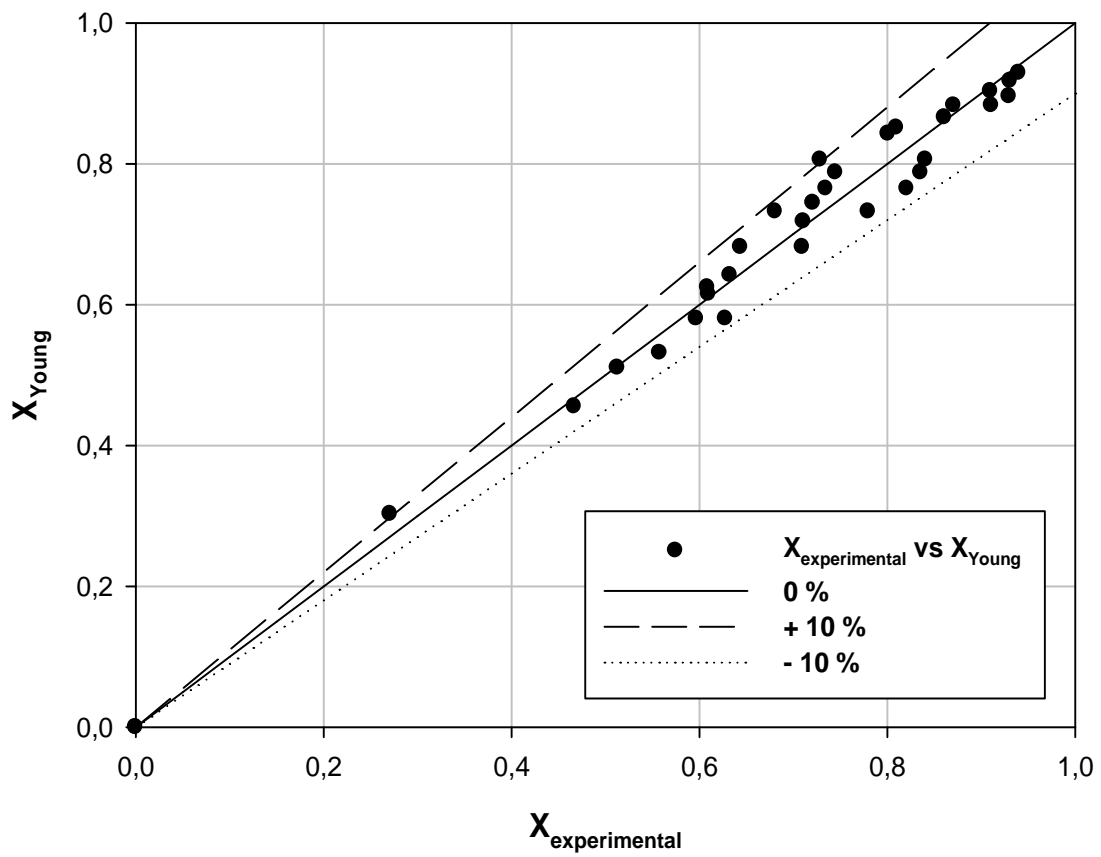


Figure 8

747
 748
 749
 750
 751
 752
 753
 754
 755
 756
 757
 758
 759
 760
 761
 762
 763